COMBUSTION CHARACTERISTICS OF DUAL SWIRL LOW NITROGEN BURNERS IN SMALL GAS BOILERS

Xiangyun Liu[1,2],*,Zhu Liang[2],LiangDe Liu[2], XiuFang Ke[2], Haitao Zheng[3]

[1.]School of Mechanical and Electrical Engineering,Guangzhou city construction college,510925,China

[2.]Department of Materials and Energy,Guangdong University of Technology,Guangzhou, 510006,China

[3.]Energy Centre, Council for Scientific and Industrial Research (CSIR), Pretoria, 0001, South Africa

[*]Corresponding author: forlxy@163.com

Swirl combustion technology is an effective method for achieving low-nitrogen (low NOx) combustion. In this study, we designed a dual-swirl low-NOx burner with the goal of minimizing NOx emissions. and the burner was evaluated in a 20t/h gas boiler through numerical simulation and experimentation. Swirl angles and excess air coefficients (1.0 to 1.20) of the burner were tested within the range of 1.0 to 1.2. The results indicated that the optimal swirl plate angles were 35° internally and 55° externally. The optimal excess air coefficient was 1.15, which balances heat transfer efficiency and minimize NOx emissions. Results show that the dual swirl combustion system can effectively reduce nitrogen oxide emissions in small gas boilers.

Keywords: Dual-swirl low-NOx burner; Gas boiler; Excess air coefficient; Central air ratio.

Nomenclature:

C_P——*specific heat capacity at constant pressure,J/(kg·K)*

E——internal energy,J

f_x,f_y,,f_z,——unit mass force in the x,y,z coordinate directions, respectively,N/kg

f_{mean}——the average mixing degree of fuel and oxidizer in turbulent flow field,(f_{mean}=1means pure fuel flow; f_{mean}=0 means pure oxidant flow);

f_{var}——the fluctuation intensity of the mixing fraction caused by turbulent fluctuations around its average value f_{mean};

K——heat transfer coefficient,W/(m·K)

k——turbulence kinetic energy

u——velocity in the x-axis direction,m/s

v——velocity in the y-axis direction,m/s

w——velocity in the z-axis direction,m/s

M——molecular weight,g/mol

p——pressure,Pa

R——gas constant

r——reaction rate,m3/s

S——resource item

t——time,s

T——temperature, K

V0——Theoretical air volume,m3

V——Actual air volume,m3

[O_2]——oxygen concentration,ppm

[N_2]——nitrogen concentration,ppm

[NO]——nitrogen oxides concentration,ppm

[fuel]——fuel concentration,ppm

Symbols：

α—— Inside spiral angle(cllockwise)，deg

β——Outside spiral angle(counterclockwise)，deg

ρ——decity,kg/m^3

ε——turbulent dissipation rate

σ——unit shearing stress,Pa·s

λ——Excess air coefficient ($\lambda = \frac{V_0}{V}$ *)*

Subscript:

x——x axis

y——y axis

z——z axis

i—— substance i

j—— substance j

1. Introduction

Industrial boilers, as crucial equipment for steam generation and water heating, play an indispensable role in industries including power generation, chemical processing, and textiles[1]. However, the emissions from these industrial boilers are among the primary contributors to climate change, with an average annual emission of approximately 130 million tons per country [2]. As industrialization advances rapidly, pollution from these emissions has become increasingly severe [3-5], leading to a heightened focus on exploring cleaner energy sources and developing more efficient, low-carbon combustion technologies [6-9]. Natural gas, which produces fewer harmful substances when burned [10], is often the preferred fuel for industrial boilers. Nevertheless, the combustion of natural gas inevitably generates nitrogen oxides (NOx). The high-temperature zones during natural gas combustion promote the formation of both fuel-bound NOx and thermal NOx through the reaction of nitrogen and oxygen in the air[11]. Nitrogen oxides emitted into the atmosphere can lead to a range of environmental issues, including the greenhouse effect, photochemical smog, and acid rain [12-13]. The NOx emission standard for gas-fired boilers is generally set at below 150 mg/m^3. Therefore, it is of great significance to study cleaner and more efficient gas boiler combustion technology. Currently, some gas-fired boiler units employ swirl combustion technology[14], which is primarily implemented through burners, making it relatively straightforward to retrofit existing gas-fired boilers.

Many researchers have been able to enhance the combustion efficiency of industrial boilers and reduce NOx emissions through the optimization of burner structural parameters and operating conditions [15-18]. In particular, studies on swirl burners have shown that the intensity of the cyclone generated by changes in burner structure affects NOx emissions and combustion performance. Zhien et al. [19] combined swirl and staged combustion theories to study and optimize the shape of new burners. Experiments by Amiri et al. [20] demonstrated that using a 60° blade angle in air swirlers and burners minimizes pollutant emissions and is optimal for achieving stable combustion and low NOx emissions. Yılmaz et al. [21]demonstrated through numerical simulations and experiments that different eddy numbers have a significant impact on the flame temperature and gas concentration of natural gas combustion. Other studies using numerical simulations have revealed that the blade angle of the swirler and the fuel equivalence ratio can significantly improve combustion performance and achieve the lowest levels of NOx emissions. Regarding the operating conditions of burners [22-25], it is essential to analyze the impact of the furnace's excess air coefficient on combustion characteristics. Jiang et al. [26], through experiments and simulations, found that increasing the excess air coefficient at semi-load conditions in a 550MW coal-fired boiler decreases the furnace temperature and significantly increases NOx emissions. Emami et al.[27]conducted a numerical simulation of the natural gas combustion process in an industrial gas turbine combustor. The results indicated that thermal NOx increases with the increase of excess air ratio. Wang et al.[28] also conducted a numerical simulation on the NOx emission characteristics in a 600MW operational boiler. The result showed that a

specific excess air coefficient can form a reducing atmosphere in the main combustion zone and effectively reduce the NOx concentrations.

Furthermore, horizontal staged combustion technology is considered as another effective way to reduce NOx emissions from boilers. Wang et al.[29] used numerical simulations to study the flow field of air-staged combustion in a decomposition furnace, and found that air staging can increase the residence time of solid particles and balance furnace temperatures. Li et al.[30] innovatively designed the secondary air and fuel pipeline structures, applied air-staged combustion technology to small and medium-sized biomass boilers, and successfully reduced NOx emissions to international standards.

Existing research on swirl burners is mostly focused on single-swirl configurations, lacking the relationship between the swirl intensity, excess air coefficient, and furnace temperature field parameters of dual-swirl burners using horizontal staged combustion [31-35]. The combustion characteristics and efficiency of these dual-swirl burners in gas boilers require further study.

In this work, a novel dual-swirl low-NOx burner is designed and Fluent is used for numerical simulations to study the effects of different internal and external swirl intensities, excess air coefficient, and air center ratio on the furnace flow field, temperature field, and NOx concentration distribution. The research results provide a reference for optimizing dual-swirl low-NOx burners for gas boilers.

2. Numerical Simulation and Computational Methods

2.1 Physical Model

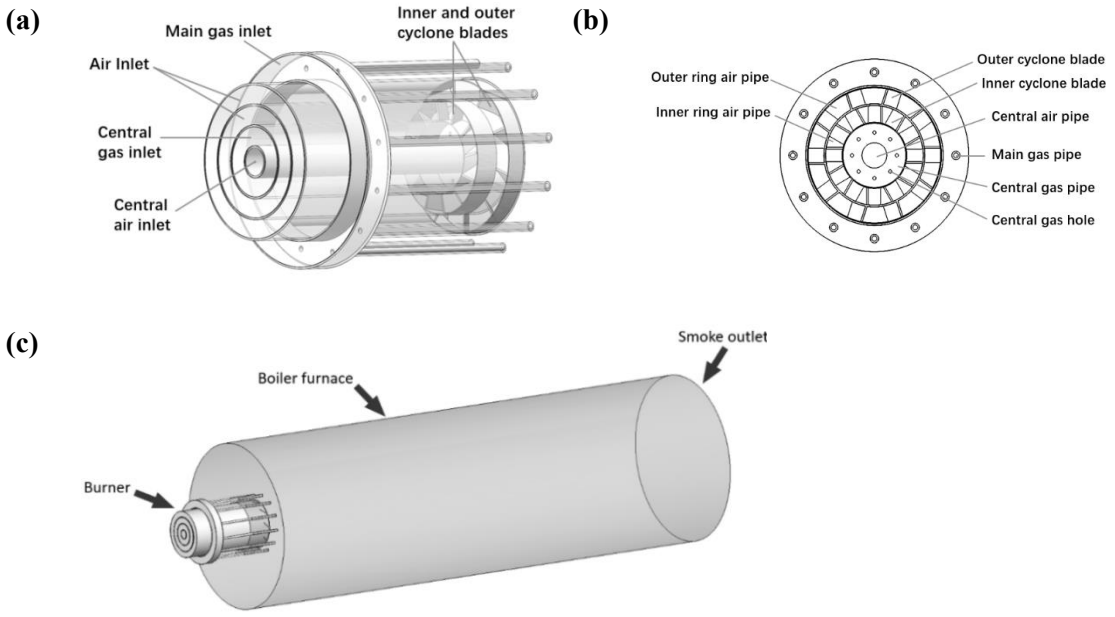

Fig. 1 Diagram of dual swirl flow burner model (a); Two-dimensional plane view of the burner (b); Three-dimensional view of the boiler model (c)

The physical model of the dual-swirl low-NOx burner is depicted in Fig.1. The uniqueness of this structure lies in the fact that, in addition to the central air and fuel, it also has dual adjustable vortex blades (for the inlet) and two layers of fuel (CH_4) inlet (the main ring of CH_4 inlet and 12 main CH_4 pipelines). Fig.1a shows a schematic diagram of dual swirl flow burner model, which includes a central air pipe, a central gas pipe, inner and outer (dual) adjustable swirl vanes(for air inlet) , the main ring of gas(CH_4) inlet, and 12 main gas(CH_4) pipes. The central air pipe's inlet injects air into the combustion chamber. The central gas pipe, sleeved around the central air pipe, has its end sealed and features 8 gas holes for injecting gas into the combustion chamber to mix with the central air. The outer and inner air pipes are also wrapped around the central gas pipe, and dual swirl formed through the inner and outer swirl vanes. The main gas annular channel is connected to the external gas pipes that inject gas into the combustion chamber and interact with the dual swirling airflow. Fig. 1b provides a 2D front view schematic of the burner, with specific parameters listed in Table S1 （Supporting information）. Fig. 1c illustrates the layout of the small gas-fired boiler furnace with a burner. The rated evaporation capacity of the boiler is 20t/h.

2. 2 Numerical Simulation Methods

In this work, control equations and several models were used as shown below:

2.2.1 Control equations

（1）Mass conservation equation:

$$\frac{\partial}{\partial x_j}(\rho u_j)=0 \qquad (1)$$

（2）Momentum conservation equations:

$$\frac{\partial(\rho u_i u_j)}{\partial x_j} = -\frac{\partial p}{\partial x_j} + \frac{\partial \tau_{ij}}{\partial x_j} + \rho f_i \qquad (2)$$

（3）Energy conservation equation:

$$\rho C_P\left(u\frac{\partial T}{\partial x} + v\frac{\partial T}{\partial y} + w\frac{\partial T}{\partial z}\right) = \nabla（K\nabla T） + S \qquad (3)$$

Where,$S = -\Delta H_r \cdot r$,ΔH_r means reaction enthalpy(J/kg); r means chemical reaction rate(kg/(m³·s)).

2.2.2 Models

2.2.2.1 Turbulence model

The realizable $k-\varepsilon$ turbulence model is used [36], which exhibits superior performance for various flow phenomena such as vortex flow, free jet and mixed flow, boundary layer flow, separation flow, etc. The transport equations of k and ε in the model are as follows:

$$\frac{\partial(\rho k)}{\partial t} + \frac{\partial(\rho k u_j)}{\partial x_j} = \frac{\partial}{\partial x_j}\left[\left(\mu + \frac{u_t}{\sigma_k}\right)\frac{\partial k}{\partial x_j}\right] + P_k + G_b - \rho\varepsilon - Y_M \qquad (4)$$

$$\frac{\partial(\rho\varepsilon)}{\partial t}+\frac{\partial(\rho\varepsilon u_j)}{\partial x_j}=\frac{\partial}{\partial x_j}\left[\left(\mu+\frac{u_t}{\sigma_\varepsilon}\right)\frac{\partial\varepsilon}{\partial x_j}\right]+\rho C_1 S_\varepsilon-C_2\rho\frac{\varepsilon^2}{k+\sqrt{v\varepsilon}}+C_{\varepsilon1}\frac{\varepsilon}{k}C_{\varepsilon3}G_b \qquad (5)$$

In the equation, C_1 =max (0.43，$\frac{\eta}{\eta+5}$), u_t represents the velocity of the fluid, whereas ρ stands for density, μ denotes dynamic viscosity, and G_b is the turbulent energy generated due to buoyancy. For incompressible fluids, G_b=0; ρε represents the dissipation term, and Y_M signifies the compressibility term. σ_k and σ_ε correspond to the source terms for equations of k and ε, respectively. $C_{\varepsilon1}\frac{\varepsilon}{k}C_{\varepsilon3}G_b$ denotes the buoyancy correction, where $C_{\varepsilon3}=\tanh\left|\frac{v_{pa}}{v_{per}}\right|$, with v_{pa} being the velocity component parallel to the gravitational direction, and v_{per} that perpendicular to the gravitational direction. In equations 6 and 7, $C_{\varepsilon1}$ is set to 1.44, C_2 to 1.92, σ_k to 1.0, and σ_ε to 1.3. P_k represents the turbulent kinetic energy generated by the mean velocity gradient, k and ε respectively denote the turbulent kinetic energy and its dissipation rate, whereas σ_k and σ_ε represent the Prandtl numbers for k and ε.

2.2.2.2 Combustion model

The combustion model adopts the Eddy-Dissipation Model (EDM) for species transport provided by Fluent. Developed jointly by Magnussen and Hjertager[37], this combustion model can simulate the chemical interactions of fluids in turbulence. The eddy-dissipation formula is as follows:

$$R_{i,r}=\bar{v}_{i,r}M_{w,i}A\rho\frac{\varepsilon}{k}\min\left(\frac{Y_R}{\bar{v}_{R,r}M_{\omega,i}}\right) \qquad (6)$$

$$R_{i,r}=\bar{v}_{i,r}M_{w,i}AB\frac{\varepsilon}{k}\left(\frac{\sum_P Y_P}{\sum_j^N \bar{v}_{j,r}M_{\omega,j}}\right) \qquad (7)$$

In the equation, $R_{i,r}$ represents the net production rate of substance i in reaction r,$\bar{v}_{i,r}$ represents the stoichiometric coefficient of reactant i in reaction r,$M_{w,j}$ represents the molecular weight of substance j, $M_{w,i}$ represents the molecular weight of substance i, Y_P represents the mass fraction of product P, Y_R represents the mass fraction of specific reactant R, and A and B represent the constants of the Eddy-Dissipation Model, where A = 4.0 and B=0.5.

2.2.2.3 Radiation model

The P-1 model is the simplest type of radiation model, considering the computational performance of the computer when running Fluent for combustion simulations. This study uses the P-1 radiation model, and its computational formula is：

$$i(s\omega)=\sum_{l=0}^{\infty}\sum_{m=-1}^{l}A_{lm}(s)Y_{lm}(\omega) \qquad (8)$$

2.2.2.4 Pollutant model

The main pollutants generated by gas boilers are nitrogen oxides（NOx）. The production of NOx includes prompt type, thermal type, and fuel type. Since the fuel used in this study is natural gas, which does not contain nitrogen elements, only the prompt type and thermal type NOx formation need to be considered in the analysis.The reaction rate equation for prompt NOx is [38]:

$$\frac{d[NO]}{dt}=f_c k_{prompt}[O_2]^m[N_2][fuel]\exp\left(\frac{E_a}{RT}\right) \qquad (9)$$

Where, m represents the oxygen reaction order, E_a stands for the activation energy; R is the universal gas constant; f_c is the correction factor depending on fuel type and air-fuel ratio; T denotes the temperature. $f_c = 4.75 + 0.0819n - 23.2\phi + 32\phi^2 - 12.2\phi^3$,and

$$k_{prompt} = 6.4\times10^6 \left(\frac{RT}{p}\right)^{a+1} \quad (10)$$

In the equation above, n represents the number of carbon atoms in the hydrocarbon fuel molecule; ϕ is the equivalence ratio; and p is the pressure. The expression for the reaction order m of the O reaction is as follows [39]:

$$m = \begin{cases} 1.0 & X_{O_2} < 4.1\times10^{-3} \\ -3.95 - 0.9\ln X_{O_2} & 4.1\times10^{-3} \le X_{O_2} < 1.11\times10^{-2} \\ -0.35 - 0.11\ln X_{O_2} & 1.11\times10^{-2} \le X_{O_2} < 3\times10^{-2} \\ 0.3\times10^{-2} \le X_{O_2} \end{cases} \quad (11)$$

In the equation, X_{O_2} corresponds to the molar fraction of O_2.

The generation rate of thermal NOx is defined as follows [38]:

$$\frac{d[NO]}{dt} = 22k_1[O][N_2]\frac{\left(1-\frac{k_{-1}k_{-2}[NO]^2}{k_1[N_2]k_2[O_2]}\right)}{\left(1+\frac{k_{-1}[NO]}{k_2[O_2]+k_3[OH]}\right)} \quad (12)$$

In the formula, k means the reaction coefficient, the expression are as follows:

k_1=1.8×10^8*exp*(-38370/*T*) , k_2=1.8×10^{4}exp(-4680/*T*) , k_3=7.1×10^{7}exp(-450/*T*) , k_{-1}=3.8×10^{7}exp(-425/*T*)，k_{-2}=1.7×10^{8}exp(-24560/*T*).

2.2.3 Boundary conditions

In this study, the numerical simulation is based on the following boundary conditions: Assuming all gases are ideal gases, the combustion reaction is a single combustion. The gas/air inlet is set as a velocity inlet with the the pipe diameter as hydraulic diameter and the turbulence intensity of 5%. The flue gas outlet is set as pressure outlet. The furnace wall adopts radiation shielding, and the isothermal wall temperature is 678K. The detailed parameters of the entrance boundary conditions of the model are shown in Table 1. In addition, the outlet pressure of the model is 2331 Pa.

Table 1 Boundary conditions

Name	Speed inlet (m/s) /Temperature (K)
Central gas inlet	3/293.15
Main gas inlet	1.6/293.15
Central air inlet	42.54/323.15
Outer ring air inlet	21.22/323.15
Inner ring air inlet	21.22/323.15

2.3 Mesh independence verification and Model validation

2.3.1 Mesh independence verification

Simulations were performed using five different mesh quantities (Table 2). The simulation results from the different mesh quantities are shown in Fig. 2.

Table 2 The number of grids for five cases

	Case1	Case2	Case3	Case4	Case5
Number of Grids（$\times 10^4$）	142	165	181	201	232

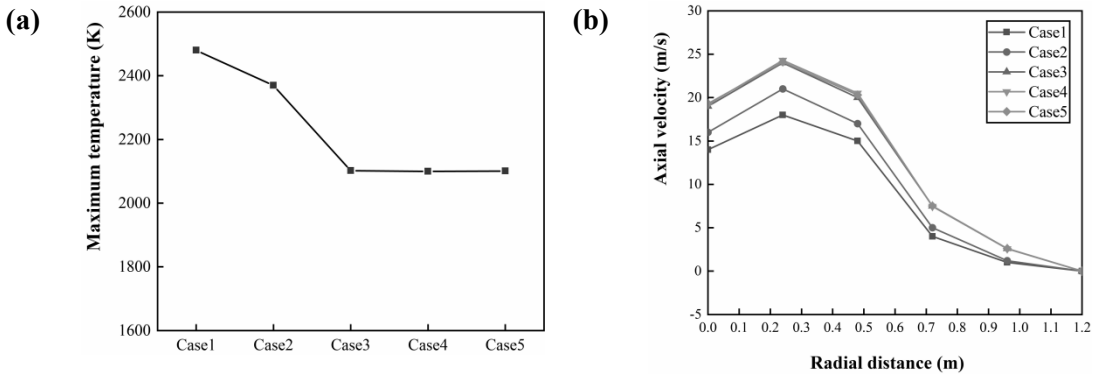

Fig. 2 Grid independent solution:(a) temperature simulation; (b) Speed simulation

Fig. 2a illustrates the highest temperature distribution inside the furnace with changes of grids numbers. It can be seen that from Case1 to Case3, as the number of grids increases, the temperature drops sharply, while from Case3 to Case5, the temperature tends to be stable. The temperatures from Case4 and Case5 are similar. Fig. 2b shows the velocity distribution at a radial distance of 6m along the axial direction with the furnace centerline as the reference, indicating similar simulation results for Case3, Case4, and Case5. Taking into account overall performance compatibility with the computer system, Case4 with a total of 2.01 million grids was ultimately selected for the simulation calculations.

2.3.2 Model validation

The experimental schematic diagram and model experiment verification is shown in Fig.3.Fig. 3a shows a schematic diagram of experimental setup where gas flow velocity and distribution inside the furnace were measured. The same operating conditions as the experiment were used to perform numerical simulation calculations using simulation software. Fig. 3b and Fig. 3c show that under the same working conditions, the maximum error between the numerical simulation results and experimental data is 8.6%, indicating a good agreement between the two sets of data. Where, Y in Fig. 3 (b) represents the radial distance from the furnace center as the origin at a distance of 0.5m from the furnace inlet; Z in Fig.3 (c) represents the central axis of the furnace, with the flow direction being the positive direction. Therefore,

the numerical simulation results obtained from the combustion numerical model established in this study are deemed reliable.

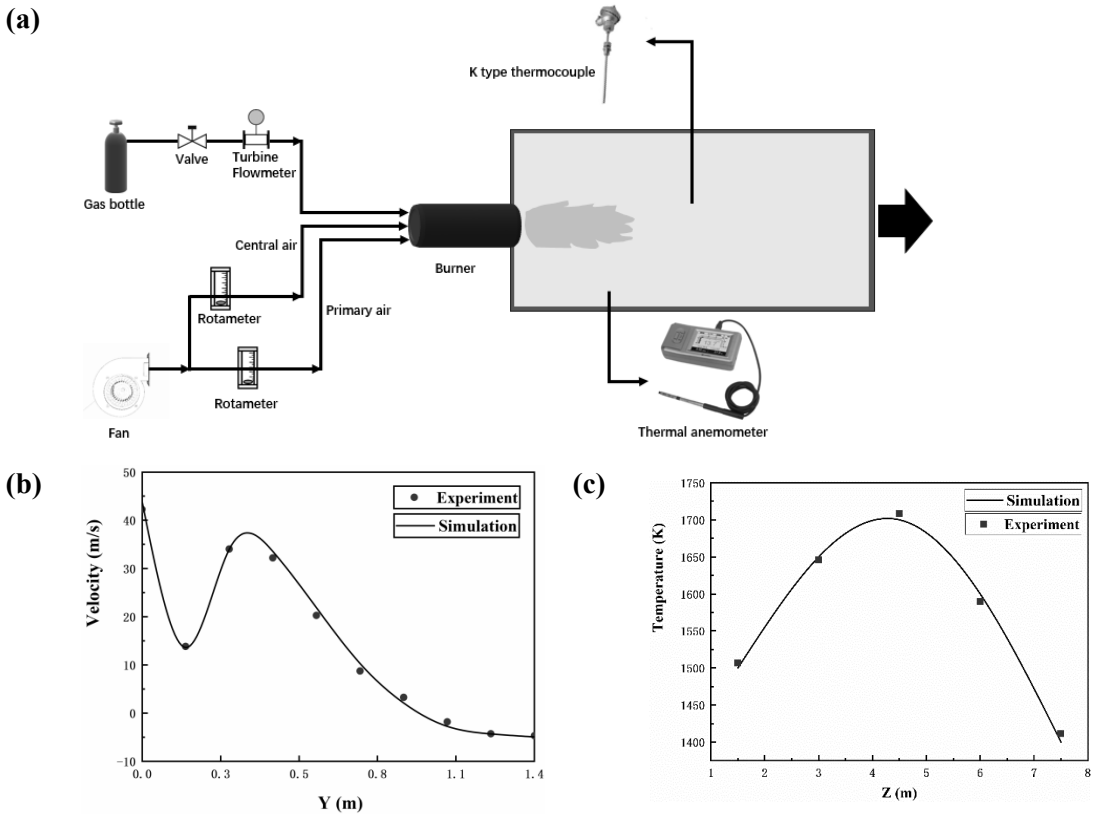

Fig. 3 Experimental schematic diagram & model experiment verification: (a) Schematic diagram of experimental (b)0.5m axial distance radial velocity (c) Comparison of experimental and simulated temperatures

3 Results and Discussion

3.1 Effects of different swirl angles on Inner and outer sides

Low-NOx burners usually use a special structure design to inject air in a swirl flow. The swirl flow can form a central recirculation zone inside the boiler, enhance the mixing of gas fuel and air in non-premixed combustion, and effectively reduce NOx emissions in the flue gas. In this paper, a dual swirler burner structure is designed, the mechanical details is shown in Fig. 4.

It is necessary to study the arrangement and deflection angles of the two layers of swirl plates and their effect on the characteristics of low-NOx combustion in gas boilers. Specifically, Table 3 lists the combination of four different swirl angles, where the inner/outer swirl angles are designated as α/β, respectively.

The temperature field, velocity field, and nitrogen oxides concentration field generated and distributed in the furnace under four different swirl angle configurations were investigated. The study conditions included an excess air coefficient of 1.0 and central air flow rate of 5%. In Table 3, the four Cases represent different configurations of α and β arrangements.

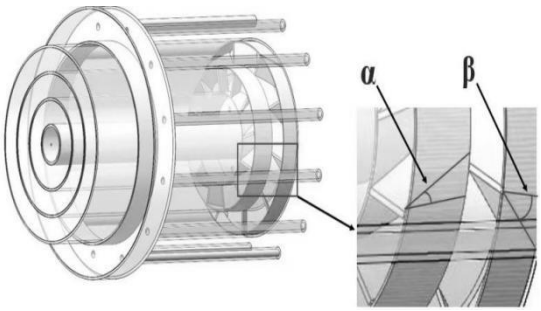

Fig. 4 Detailed geometric structure of dual swirl low nitrogen burner

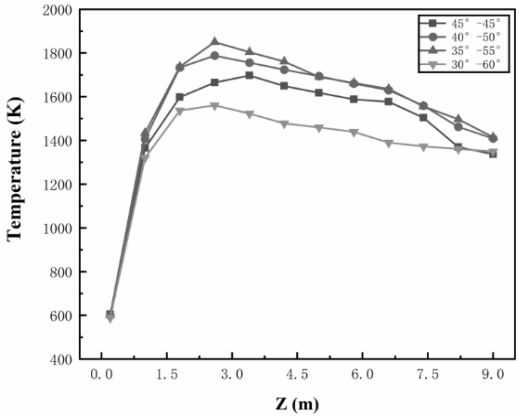

Fig. 5 Average temperature with different swirl angle arrangements

Table 3 Spiral Angle Arrangement and Coordination

Case	α°	β°	layout direction
1	30	60	Clockwise inside, counterclockwise on the outside
2	35	55	
3	40	50	
4	45	45	

When the heat transfer pipes of the gas boiler are dry, the average temperature curves with different swirl angles are shown in Fig.5 (Z-axis is represented as the axial distance distributed along the central axis of the furnace, with the flow direction being the positive direction, X-axis represent the width of the burner). It can be observed that the temperature trends of different operating conditions are similar, all of which rise sharply first and then fall slowly. As gas and air mix rapidly at the front end of the furnace, the temperature rises sharply. Next, the high-temperature fluid produced by combustion undergoes heat exchange along the furnace wall. When α=35° and β=55°, the temperature peak reaches 1850K, and the overall average temperature is also higher than that of other configurations. Therefore, when α=35° and β=55°, the mixed combustion efficiency of gas and air in the double-swirl burner is highest.

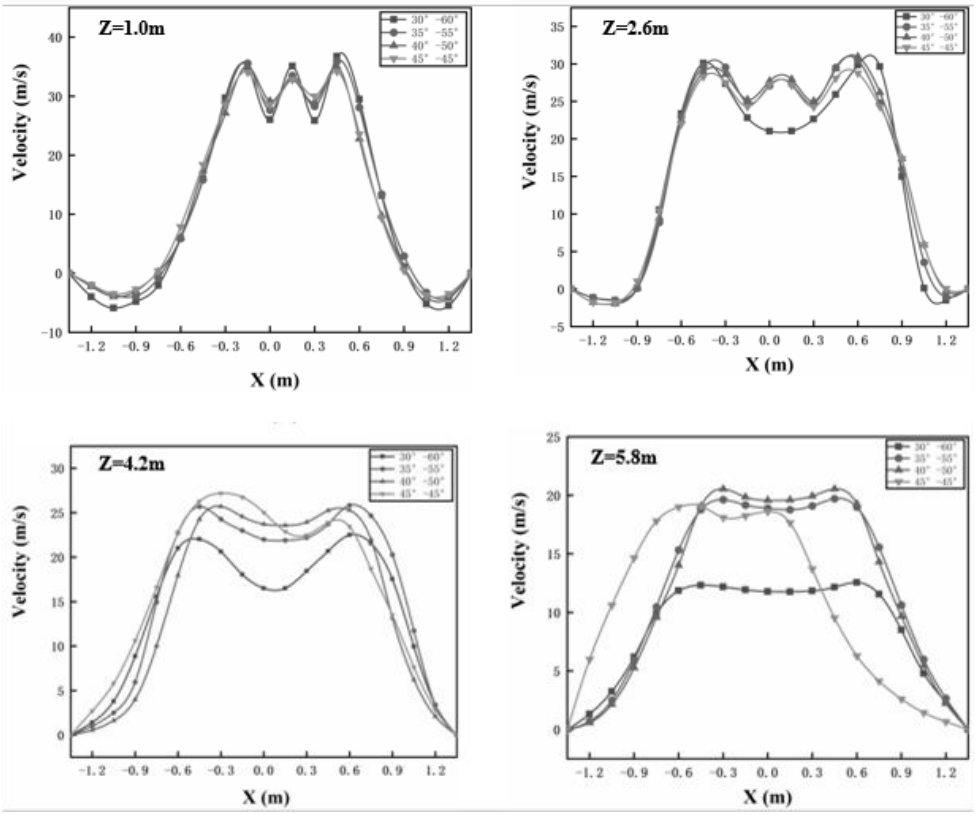

Fig. 6 Velocity distribution with different swirl angles at different axial distances

For the four swirl angle schemes, Fig. 6 shows variations in radial velocity distribution at furnace cross-sections located at 1.0m, 2.6m, 4.2m, and 5.8m from the central axis. As the distance Z from the cross-section increases, the velocity distribution changes from wavy to smooth. Recirculation zones are observed at Z=1.0m and Z=2.6m. Case 1 shows a significant difference from others since Z=1.0m. Due to the excessive intensity of the external swirl flow, the airflow is concentrated in the front of the furnace, so the airflow velocity shown at Z=4.2 and Z=5.8 is lower than that of the others for Case 1. However, Case 4 exhibits an asymmetrical high-speed gas distribution at Z=4.2 and Z=5.8, likely due to insufficient swirl intensity, leading to inadequate axial velocity for uniform distribution at the furnace's rear, which hampers heat exchange. With the distance of Z increases, the kinetic energy of the airflow in all cases decreases, and the axial airflow velocity gradually decreases, resulting in a smoother distribution in the rear. However, cases 2 and case3 can still maintain turbulence and the mixture gas uniformity. Therefore, the optimal velocity field distribution within the furnace occurs when the swirl vanes have dual-swirl angles of α=35° and β=55°, or α=40° and β=50°.

From the velocity distribution shown in Fig. 7a, As the angle between the inner and outer vortices decreases, the central velocity of the flue gas in the furnace increases, and the turbulence effect is enhanced. This is because if excessive deflection of the swirl vanes is too large, the tangential velocity of the air flow ejected by the burner will be reduced. Conversely, the deflection of the vanes is too small, the flow disturbance effect of the dual swirl will not be obvious.

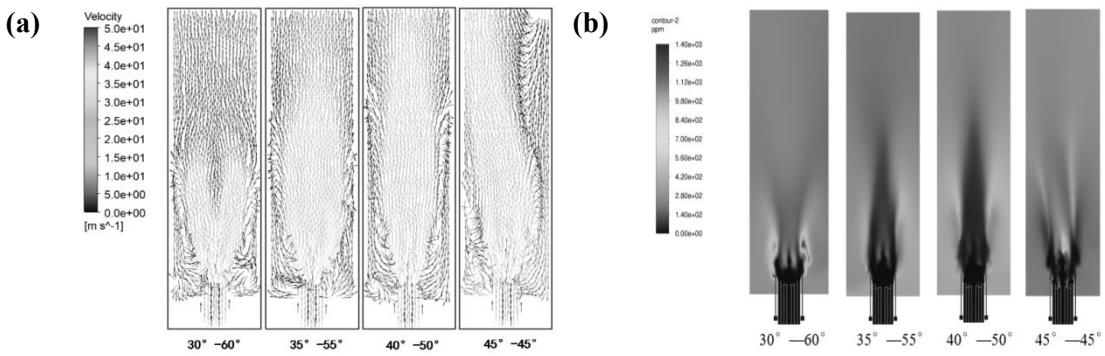

Fig. 7 Velocity vector and nitrogen oxide distribution inside the furnace at different swirl angles:(a) Velocity vector diagram;(b) Cloud map of nitrogen oxide distribution.

In Fig. 7b, it can be observed that NOx is mainly generated in the power combustion zone. The lowest nitrogen oxide outlet concentration in Case2 is 276ppm; The nitrogen oxide emission concentration of other schemes is around 300ppm. This is because the nitrogen oxides generated during the combustion process are mainly thermal nitrogen oxides (produced in high-temperature regions above 1100 K). The more uniform the distribution of furnace combustion temperature, the fewer concentrated high-temperature areas, and the lower the concentration of nitrogen oxides. When the internal and external swirl angles of the dual swirl burner are between 35° -55° , the minimum nitrogen oxide outlet concentration is 276 ppm. The results indicate that the optimal swirl arrangement is achieved when the swirl angles α =35° and β =55° .

3.2 Effects of different excess air coefficients

The excess air coefficient (λ) refers to the ratio of actual air volume(V) to theoretical air volume(V_0) ($\lambda = V/V_0$), and its magnitude has multiple effects on the combustion process of natural gas. If the excess air coefficient (λ) is too large, it will lower the flame temperature (as heat is absorbed by excess air), and sufficient oxygen may cause NOx emissions to peak, leading to a decrease in combustion efficiency and even flameout. If λ is too small, incomplete combustion will intensify, generating a large amount of CO and carbon black, significantly reducing combustion efficiency, and possibly damaging equipment due to carbon deposition.

The following section investigates the distribution of temperature field, velocity field, and nitrogen oxide concentration inside the furnace under the conditions of α =35 ° and β=55 ° , with a central air flow rate of 5% and excess air coefficients of 1.0, 1.05, 1.10, 1.15, and 1.20.

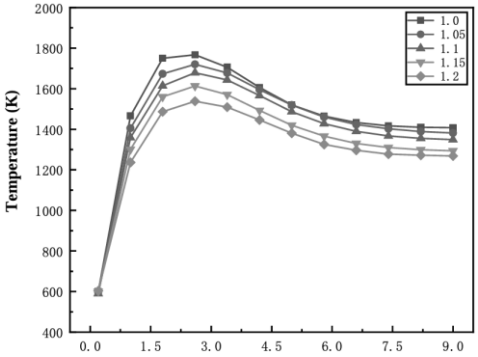

Fig. 8 The average temperature distribution with different excess air coefficients

When the heat transfer pipes of the gas boiler are full of water, the average temperature curves at different excess air coefficients are shown in Fig. 8. It can be seen that with the increase of excess air coefficient, the temperature change trend is similar, first sharply rising, then slowly falling, and finally stabilizing. This indicates that increasing the excess air coefficient is beneficial for heat exchange inside the furnace. In addition, a large amount of excess air inside the furnace will absorb the heat generated by the combustion reaction, resulting in an overall decrease in furnace temperature.

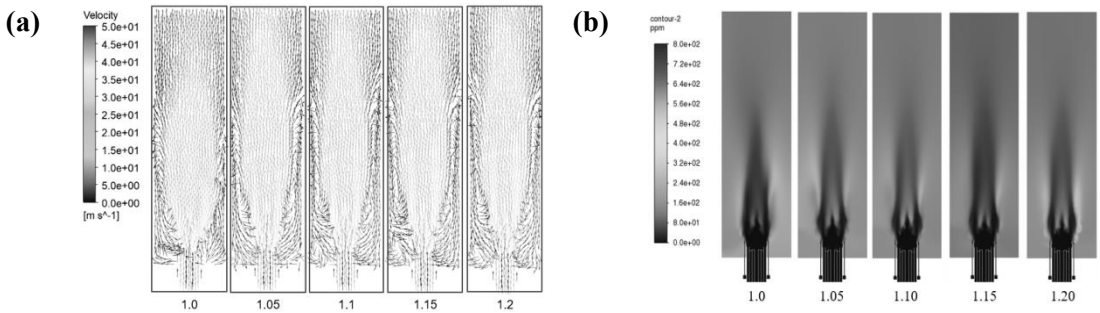

Fig. 9 Velocity vector diagram and nitrogen oxide distribution cloud map inside the furnace with different excess air coefficients:(a) Velocity vector diagram;(b) Cloud map of nitrogen oxide distribution.

Fig. 9a illustrates the distribution of gas flow velocity inside the furnace at different excess air coefficients. The gas flow velocity at the front end of the furnace increases with the increase of excess air coefficient. Since the gas inlet velocity and the burner inlet area remain unchanged, increasing the excess air coefficient can only increase the flow velocity of the combustion air. Therefore, the flow velocity of the gas at the front end of the furnace will increase, but the overall distribution of velocity will not change significantly. Fig. 9b shows the distribution of NOx at different excess air coefficients. As the excess air coefficient increases from 1.0 to 1.15, NOx concentration decreases. This reduction is likely due to improved mixing of gas fuel and air, which reduces the temperature concentration area in the furnace, subsequently decreasing the average furnace temperature and reducing formation of thermal NOx. Additionally, the increase in excess air will dilute the NOx concentration. but when the excess air coefficient increases from 1.15 to 1.2, NOx concentration begins to rise. This is because the increase in oxygen concentrations in the furnace accelerates NOx formation reactions. Considering furnace heat transfer conditions and outlet NOx concentration, the optimal excess air coefficient is 1.15.

4 Conclusion

This paper investigates the effect of various swirl cooperation angles on the combustion characteristics of a custom-designed dual-swirl burner in a gas boiler using numerical simulations. Based on the identified optimal cooperation angle, the study further explores the influence of the burner’s air excess ratio and central air ratio on combustion characteristics within the furnace. The key findings are summarized as follows:

(1) The ideal configuration of the dual-swirl burner requires precise coordination between the internal and external swirl plate angles. Neither a significantly larger nor smaller angle difference is inherently better.

(2) The optimal angles, identified as $\alpha = 35°$ and $\beta = 55°$, and this design can obtain uniform temperature distribution, maximum combustion efficiency, and lowest NOx emission.

(3) An excess air coefficient of 1.15 is optimal number for best balance and optimizing both combustion efficiency and NOx levels.

Acknowledgments

This research is financially supported by Guangzhou Science and technology planning project (2023B04J0022) and (2023B04J0037), and by by 2024 Key Field of Ordinary Universities in Guangdong Province 2024 (No. 2024ZDZX3097).

References

(1) Shen, B.,Han, Y.F., Price, L., Lu, H.Y., Liu, M.Z., 2017. Techno-economic evaluation of strategies for addressing energy and environmental challenges of industrial boilers in China. Energy 118, 526–533.
(2) Klimont, Z., et al. "Global Gridded Anthropogenic Emissions of Air Pollutants and Methane for the Period 1990-2050." IIASA.
(3) IEA, “Global energy review: CO2 emissions in 2020″, 2021-3-2.
(4) National Bureau of Statistics. Total energy consumption [EB/OL]. 2021. -11-29 [2022-10-24].
(5) Mikhaylov, A.; Moiseev, N.; Aleshin, K.; Burkhardt, T. 2020. Global climate change and greenhouse effect, Entrepreneurship and Sustainability Issues 7(4): 2897-2913.
(6) Liu X, Zhao D, Guan D, Becker S, Sun D, Sun X. Development and progress in aeroacoustics noise reduction on turbofan aeroengines. Prog Aerosp Sci 2022;130: 100796.
(7) Cardoso J, Silva V, Rocha R, Hall M. Ammonia as an energy vector: current and future prospects for low-carbon fuel applications in internal combustion engines. J Clean Prod 2021;2296:126562.
(8) Xu Y, Chang G, Fan R, Cai T. Effects of various operating conditions and optimal ionomer-gradient distribution on temperature-driven water transport in cathode catalyst layer of PEMFC. Chem Eng J 2023;451:138924.
(9) Belver C, Bedia J, G´omez-Avil´es A, Pe˜nas-Garz´on M, Rodriguez JJ. Semiconductor photocatalysis for water purification. Nanoscale materials in water purification. Elsevier; 2019. p. 581–651.
(10) S.Y. Zhang, X.L. Wang, Y. Li, W.Q. Wang, W.T. Li, Study on a novel district heating system combining clean coal-fired cogeneration with gas peak shaving, Energy Convers. Manag. 203 (2020), 112076.

(11) Wai Siong Chai, Yulei Bao, Pengfei Jin, Guang Tang, Lei Zhou,A review on ammonia, ammonia-hydrogen and ammonia-methane fuels,Renewable and Sustainable Energy Reviews,Volume 147,2021,111254
(12) Yi Jin, Laura Scherer, Edwin H. Sutanudjaja, Arnold Tukker, Paul Behrens,Climate change and CCS increase the water vulnerability of China's thermoelectric power fleet,Energy,Volume 245,2022,123339.
(13) Yu Jiang, Byoung-Hwa Lee, Dong-Hun Oh, Chung-Hwan Jeon,Influence of various air-staging on combustion and NOX emission characteristics in a tangentially fired boiler under the 50% load condition,Energy,Volume 244, Part B,2022,123167.
(14) D.J. Wang,Z.N Yang,S M Ran, et al. Numerical calculation research and application of low-load stable combustion technology for low-quality coal [J]. Clean Coal Technology, 2023,29 (S2): 181-187.
(15) Leu,J.H.2011.3D Numerical Combustion Simulation of Designed Low Heating Value Fuel Combustor for Further Detail Modulation,Advanced Materials Research,268-270,494-500.
(16) Kun Su, Ziqu Ouyang, Hongshuai Wang, Hongliang Ding, Comparative analysis on pulverized coal combustion preheated by self-sustained purifying burner with coaxial and centrosymmetric air nozzle structures: Purification, combustion and NOx emission characteristics,Chinese Journal of Chemical Engineering,2024.
(17) Xianqiang Su, Qingyan Fang, Lun Ma, Bin Yao, Yuan Li, Xinping Zhao, Rui Mao, Chungen Yin,Improving combustion and lowering NOx emissions of an industrial coal swirl burner by optimizing its nozzle structure,Applied Thermal Engineering,Volume 218,2023,119340.
(18) H. Zhou, Y. Yang, H. Liu, et al.Numerical simulation of the combustion characteristics of a low NOx swirl burner: Influence of the primary air pipeFuel, 130 (2014), pp. 168-176.
(19) Zhien CY, Al-attab KA. Design optimization of trio concept combustor geometry for low-grade biomass producer gas combustion. Energy 2022;238:121705.
(20) Amiri M, Shirneshan A. Effects of air swirl on the combustion and emissions characteristics of a cylindrical furnace fueled with diesel-biodiesel-n-butanol and diesel-biodiesel-methanol blends. Fuel 2020;268:117295.
(21) Yılmaz, İ. (June 24, 2013). "Effect of Swirl Number on Combustion Characteristics in a Natural Gas Diffusion Flame." ASME. J. Energy Resour. Technol. December 2013; 135(4): 042204.
(22) Jing L, Zhao J, Wang H, Li W, Du Y, Zhu Q, et al. Numerical analysis of the effect of swirl angle and fuel equivalence ratio on the methanol combustion characteristics in a swirl burner. Process Saf Environ Prot 2022;158:320–30.
(23) Darbandi M, Fatin A, Bordbar H. Numerical study on NOx reduction in a large-scale heavy fuel oil-fired boiler using suitable burner adjustments. Energy 2020;199: 117371.
(24) Z. Chen, H.Chen, L. Wang, et al.Parametric study on effects of excess air/fuel ratio, spark timing, and methanol injection timing on combustion characteristics and performance of natural gas/methanol dual-fuel engine at low loads.Energy Convers. Manag.,210 (112742) (2020)
(25) Y. Wang, X. Li, T. Mao, P. Hu, X. Li, G. WangMechanism modeling of optimal excess air coefficient for operating in coal fired boilerEnergy, 261 (2022), Article 125128.
(26) Jiang Yu, Lee B-H, Oh D-H, Jeon C-H. Optimization of operating conditions to achieve combustion stability and reduce NOx emission at half-load for a 550-MW tangentially fired pulverized coal boiler. Fuel 2021;306:121727.
(27) Emami, M. D., Shahbazian, H., and Sunden, B. (July 23, 2018). "Effect of Operational Parameters on Combustion and Emissions in an Industrial Gas Turbine Combustor." ASME. J. Energy Resour. Technol. January 2019; 141(1): 012202.
(28) Yongqiang Wang, Yuegui Zhou,Numerical optimization of the influence of multiple deep air-staged combustion on the NOx emission in an opposed firing utility boiler using lean coal,Fuel,2020; 269:116996.
(29) Weishu W , Yihan L , Jun L ,et al.Numerical Simulation and Optimization of Staged Combustion and NO_x Release Characteristics in Precalciner[J]. Journal of Thermal Science: English Edition, 2019,

28(5):11.
(30) Li Y, Lin Y, Zhao J, et al. Control of NOx emissions by air staging in small- and medium-scale biomass pellet boilers[J]. Environmental Science and Pollution Research(2019).
(31) Y. Wang, Y. Zhou Numerical optimization of the influence of multiple deep air-staged combustion on the NOx emission in an opposed firing utility boiler using lean coal Fuel, 269 (2020), Article 116996.
(32) L. Zhao, Q. Zhou, C. Zhao Flame characteristics in a novel petal swirl burner Combust. Flame, 155 (1) (2008), pp. 277-288.
(33) Z. Chen, Z. Li, Q. Zhu, et al. Gas/particle flow and combustion characteristics and NOx emissions of a new swirl coal burner.Energy, 36 (2) (2011), pp. 709-723.
(34) S. Xue, S. Hui, Q. Zhou, et al. Experimental study on NOx emission and unburnt carbon of a radial biased swirl burner for coal combustion. Energy Fuels, 23 (4) (2009), pp. 3558-3564.
(35) S. Ti, Z. Chen, Z. Li, et al. Effect of outer secondary air vane angles on combustion characteristics and NOx emissions for centrally fuel rich swirl burner in a 600-MWe wall-fired pulverized-coal utility boiler.Appl. Therm. Eng., 125 (2017), pp. 951-962.
(36) Chakchak S, Hidouri A, Ghabi A, Chrigui M, Boushaki T. Numerical study of turbulent swirling diffusion flame under lean and rich conditions using turbulence realizable k-epsilon model. Combust Sci Technol 2023;195(7):1461 – 82.
(37) B.F. Magnussen, B.H. Hjertager, On mathematical modeling of turbulent combustion with special emphasis on soot formation and combustion, Symp. Combust. 16 (1) (1977) 719 – 729.
(38) F. Bachmaier, K.H. Eberius, T. Just, The formation of nitric oxide and the detection of HCN in premixed hydrocarbon-air flames at 1 atmosphere, Combust Sci Technol, 7 (2) (1973) 77 – 84.
(39) G.G. de Soete, Overall reaction rates of NO and N2 formation from fuel nitrogen, Proc. Combust. Inst. 15 (1993) 1093 – 1102.

Received: 26.3.2025.

Revised: 13.8.2025.

Accepted: 14.8.2025.